A Comparison of Strategies for Managing Energy Constraints of Energy Storage Providing Frequency Regulation

Hannah Moring
Electrical Engineering & Computer Science
University of Michigan
hmoring@umich.edu

Johanna L. Mathieu
Electrical Engineering & Computer Science
University of Michigan
jlmath@umich.edu

Abstract

CAISO and PJM operate the majority of grid-connected batteries in the U.S. The two markets manage the energy constraints of batteries providing frequency regulation differently. PJM, which has a fast (RegD) and a slow (RegA) regulation signal, uses RegA to conditionally maintain energy neutrality of the RegD signal over short durations. CAISO offsets net energy produced/consumed for frequency regulation with energy from the real-time energy market. This paper presents a comparison of these strategies with the goal of assessing the advantages and disadvantages of each approach. Specifically, we compare the approaches in terms of regulation signal-following performance and additional system control effort. Case study results suggest that both strategies can reliably keep a battery away from its state of charge limits but that PJM's strategy requires larger energy deviation from base operations.

1. Introduction

Growing reliance on intermittent and uncertain renewable energy generation has led to increase in demand for energy storage, a trend which is expected to continue [1]. Energy storage, specifically battery energy storage systems (henceforth simply batteries), can provide many services to the grid including but not limited to arbitrage, peak shaving, and frequency regulation [2]. Federal Energy Regulatory Commission (FERC) orders in the last 11 years have led to increased participation of batteries in energy markets. Most notably are FERC Order 755 (issued in 2011), which requires markets to compensate for resources that can provide faster-ramping frequency regulation, and FERC order 841 (issued in 2018), which requires system operators to remove barriers for batteries and similar resources to participate in the capacity, energy, and ancillary services markets [1].

This work was supported by NSF Grant 1845093.

In response to FERC Order 755, the PJM Interconnection (PJM) split its frequency regulation service into a faster-ramping service (RegD), well-suited to batteries, and a slower-ramping service (RegA). Within a few years, more than 180 MW of large-scale battery power capacity had been installed in PJM [1], far outpacing the installation rate in other U.S. markets. The California Independent System Operator (CAISO) also experienced a large influx of battery power capacity after the California Public Utility Commission passed an energy storage mandate in 2013 requiring investor-owned utilities to procure 1,325 MW of energy storage by 2020 [1]. By the end of 2020, California had 520 MW of large-scale batteries in operation, making CAISO the U.S. electricity market with the largest battery power capacity [1].

Batteries can respond faster than conventional power plants that traditionally provide frequency regulation, making them desirable for providing frequency regulation [3, 4]. However, a key challenge to using energy storage for frequency regulation is the need to manage its energy constraints [5]. Conventional power plants have power and ramping constraints, but can generally provide frequency regulation continuously over long periods so long as they are dispatched within (i.e., not at the edges of) their operational range and the offered frequency regulation capacity respects their ramping constraints. In contrast, energy storage is energy-limited meaning that it can not continuously discharge without charging, and vice versa. This means that a consistently-biased regulation signal will cause the the storage to fill or empty, making it unable to provide frequency regulation. If the regulation signal is approximately energy neutral, i.e., the energy embodied within up regulation matches the energy embodied within down regulation, over short durations then energy storage can continually provide frequency regulation. Some independent system operators (ISOs) have developed mechanisms to achieve energy neutrality in batteries providing frequency regulation; however, they all do this differently.

URI: https://hdl.handle.net/10125/102968
978-0-9981331-6-4

The objective of this paper is to compare the strategies used by PJM and CAISO for managing the energy constraints of batteries providing frequency regulation in order to assess the advantages and disadvantages of each approach. PJM employs a conditional neutrality controller, where energy used to provide fast frequency regulation by RegD resources (i.e., fast-ramping resources like batteries) is compensated by RegA resources (i.e., traditional, slow-ramping resources like conventional power plants) when there is sufficient capacity to do so [6]. Both signals capture up and down regulation. In CAISO, batteries are categorized as non-generator resources (NGRs), meaning they have the capability to serve as both generation and load but are constrained by energy limits [7]. NGRs providing frequency regulation that wish to increase their regulation capacity can opt into regulation energy management (REM). In REM, the system operator is responsible for maintaining a preferred state of charge (SoC) by offsetting net energy produced/consumed by the resource for frequency regulation with energy from the real-time market [8]. CAISO uses one signal for up regulation and one signal for down regulation.

Different frequency regulation implementations and strategies for managing the energy constraints of batteries can lead to different operational outcomes. For example, PJM redesigned their regulation controller in 2016 because their old controller often caused batteries to move in the opposite direction to that needed to regulate frequency [6]. This resulted in the need to compensate the batteries' actions through more frequency regulation control effort and more frequency regulation capacity. Overall, the design of the regulation controller should balance performance and control effort, both of which impact the required frequency regulation capacity. Improving performance can improve frequency quality and decrease the system regulation requirement [9]. Achieving better frequency quality with less regulation capacity will be increasingly important as renewable generation increases [10]. Frequency regulation implementations and strategies for managing the energy constraints of batteries can also affect other reliability and cost metrics. Understanding these trade-offs will allow ISOs to make better decisions.

The main contribution of this paper is a comparison of the strategies used by PJM and CAISO for managing the energy constraints of batteries providing frequency regulation. We quantitatively compare the strategies in terms of regulation signal-following performance and additional system control effort. To do this, we implement both regulation controllers and develop an approach to simulate the key aspects of both strategies on the PJM 5-bus system leveraging a real area control error (ACE) data. Note, this paper does not attempt to model all details of the PJM and CAISO markets, but rather we model their strategies for managing the energy constraints of batteries providing frequency regulation.

Section 2 presents mathematical descriptions of the regulation controllers. Section 3 develops the simulation method used to compute the comparison metrics. Section 4 presents our case study. Conclusions are given in Section 5.

2. Regulation Controllers

This section presents the controllers used to generate the PJM and CAISO regulation signals and, for CAISO, the method of calculating the energy offset needed for REM.

2.1. PJM Conditional Neutrality Controller

Here we present a mathematical representation of the PJM conditional neutrality controller and briefly summarize its key features, as described in [6]. PJM generates two types of regulation signals. The RegA signal is designed for slower-ramping resources, and the RegD signal is designed for faster-ramping, energy-limited resources. Both signals are bi-directional with symmetric limits; a negative signal represents down regulation and a positive one represents up regulation.

The controller, shown in Fig. 1, uses proportional-integral (PI) control with an internal feedback loop which controls the SoC of resources providing RegD. The input to the controller is the ACE, which is multiplied by -1 to obtain the ACE correcting signal (ACS). To create the RegA signal, the ACS is passed through the PI controller, combined with the accumulated neutrality bias $B(s)$ (described later), passed through a low-pass filter, and finally constrained to have a magnitude less than or equal to the total RegA capacity via a saturation filter $\mathrm{sat_A}$. Mathematically,

$$\mathrm{RegA}(s) = \mathrm{sat_A}\left(\frac{-\mathrm{ACE}(s)\left(\frac{K_\mathrm{I}}{s} + K_\mathrm{P}\right) + B(s)}{\tau_\mathrm{A} s + 1}\right), \tag{1}$$

where $\mathrm{ACE}(s)$ is the ACE signal, K_P and K_I are the proportional and integral control gains of the PI controller, τ_A is the time constant of the low-pass filter that reflects the ramping constraints of the generators providing RegA, and

$$\mathrm{sat_A}(x) = \begin{cases} x, & \text{if } -\overline{\mathrm{RegA}} \le x \le \overline{\mathrm{RegA}}, \\ \overline{\mathrm{RegA}}, & \text{otherwise}, \end{cases} \tag{2}$$

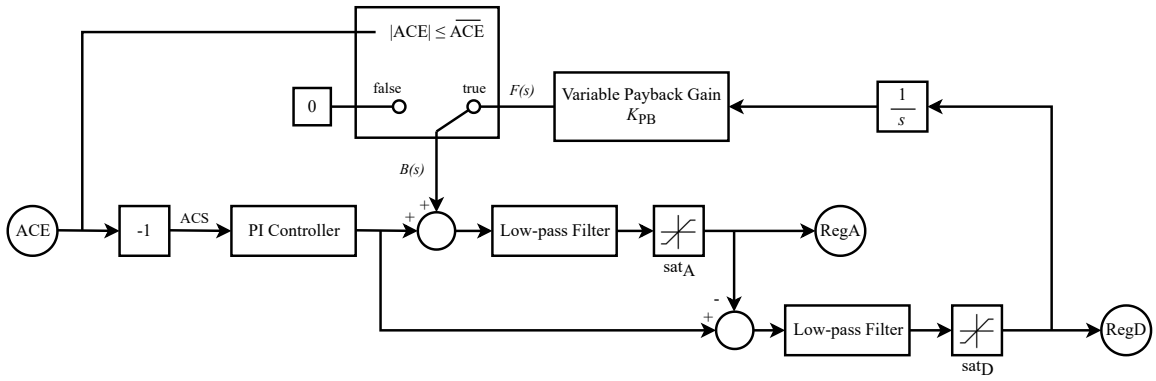

Figure 1. Block diagram for PJM conditional neutrality controller.

where $\overline{\mathrm{RegA}}$ is the capacity for RegA.

The residual between the output of the PI controller and the RegA signal is passed through another low-pass filter and constrained to have a magnitude less than or equal to the total RegD capacity via a saturation filter $\mathrm{sat_D}$, resulting in the RegD signal

$$\mathrm{RegD}(s)=\mathrm{sat_D}\left(\frac{-\mathrm{ACE}(s)\left(\frac{K_\mathrm{I}}{s}+K_\mathrm{P}\right)-\mathrm{RegA}(s)}{\tau_\mathrm{D}s+1}\right), \tag{3}$$

where τ_D is the time constant of the low-pass filter that reflects the faster but still limited ramping constraints of the resources providing RegD and

$$\mathrm{sat_D}(x)=\begin{cases} x, & \text{if } -\overline{\mathrm{RegD}} \le x \le \overline{\mathrm{RegD}}, \\ \overline{\mathrm{RegD}}, & \text{otherwise}, \end{cases} \tag{4}$$

where $\overline{\mathrm{RegD}}$ is the capacity for RegD.

To determine the accumulated neutrality bias, the RegD signal is first integrated to capture the net injection or withdrawal of energy over time and multiplied by a variable payback gain K_PB (described later), i.e.,

$$F(s)=\frac{K_\mathrm{PB}\cdot\mathrm{RegD}(s)}{s}. \tag{5}$$

Then, the accumulated neutrality bias is set to $F(s)$ when the magnitude of the ACE signal at or below a designated threshold $\overline{\mathrm{ACE}}$, i.e.,

$$B(s)=\begin{cases} F(s), & \text{if } |\mathrm{ACE}(s)| \le \overline{\mathrm{ACE}}, \\ 0, & \text{otherwise}. \end{cases} \tag{6}$$

When the ACE is above $\overline{\mathrm{ACE}}$, neutrality feedback is suspended. Note that both signals are unaffected by neutrality feedback when the RegA signal is at either of its limits.

Consider a single battery providing frequency regulation. The variable payback gain increases as the battery SoC deviates from 50%. In other words, the closer the battery gets to its energy limits, the further the RegA signal is pushed from the ideal control point, allowing the RegD signal to move in the direction that corrects SoC. The payback gain is calculated as

$$K_\mathrm{PB}=\begin{cases} \frac{E_\mathrm{B}}{2}, & \text{if } 37.5\% \le \mathrm{SoC} \le 62.5\%, \\ 10E_\mathrm{B}, & \text{if } \mathrm{SoC} \le 25\% \vee \mathrm{SoC} \ge 75\%, \\ \frac{60E_\mathrm{B}}{28}, & \text{otherwise}, \end{cases} \tag{7}$$

where E_B is the energy capacity of the battery in MWh. The payback gain is set to restore the SoC back to 50% within 15 min if the first condition holds, 3 min if the second holds, and 7 min if the third holds. The battery SoC is estimated using the integral of the RegD signal [11].

2.2. CAISO Regulation Signals and REM

Here we present a mathematical representation of CAISO's regulation signal generator and REM strategy. A block diagram of the controller is given in Fig. 2. Like PJM, CAISO uses PI control, low pass filtering, and generates two regulation signals [12]. However, CAISO splits its regulation signal into an up and a down regulation signal, not a fast and slow regulation signal like PJM. The up regulation signal is positive and tells participating resources to increase their power output, or to produce power in the case of a battery. The down regulation signal is negative and tells participating resources to decrease their power output, or to consume power in the case of a battery. The up and down

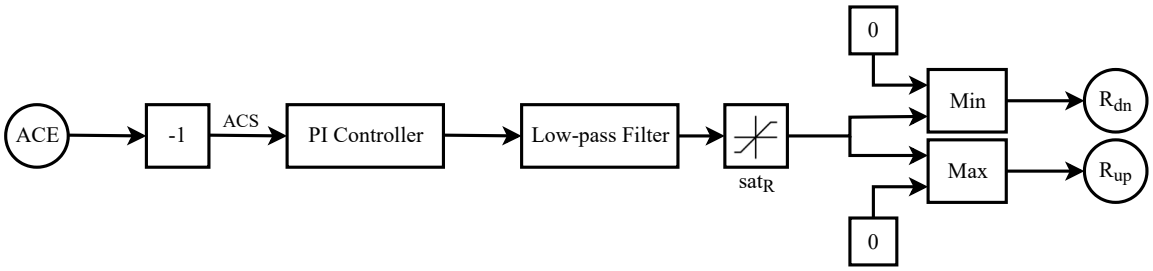

Figure 2. Block diagram of controller to generate CAISO regulation up and down signals.

regulation signals are given by

$$\mathrm{R_{up}}(s) = \max\left(0, \mathrm{sat_R}\left(\frac{-\mathrm{ACE}(s)\left(\frac{K_\mathrm{I}}{s}+K_\mathrm{P}\right)}{\tau s+1}\right)\right) \tag{8}$$

$$\mathrm{R_{dn}}(s) = \min\left(0, \mathrm{sat_R}\left(\frac{-\mathrm{ACE}(s)\left(\frac{K_\mathrm{I}}{s}+K_\mathrm{P}\right)}{\tau s+1}\right)\right) \tag{9}$$

where τ is the time constant of the low-pass filter and the saturation function $\mathrm{sat_R}$ is

$$\mathrm{sat_R}(x) = \begin{cases} x, & \text{if } -\overline{\mathrm{R_{dn}}} \le x \le \overline{\mathrm{R_{up}}}, \\ -\overline{\mathrm{R_{dn}}}, & \text{if } x < -\overline{\mathrm{R_{dn}}}, \\ \overline{\mathrm{R_{up}}}, & \text{if } x > \overline{\mathrm{R_{up}}}, \end{cases} \tag{10}$$

where $\overline{\mathrm{R_{up}}}$ and $\overline{\mathrm{R_{dn}}}$ are the total up and down regulation capacities, respectively.

To manage the energy constraints of batteries providing frequency regulation, CAISO uses the battery's current energy level and previous REM energy offsets to decides the REM energy offset for the next real-time market period [8]. CAISO's real-time market operates every 5 min.

First, the net energy produced/consumed for frequency regulation by battery i is

$$E_{\mathrm{NET},i}(s) = \frac{\left(\eta_i \cdot \gamma_{\mathrm{dn},i} \cdot \mathrm{R_{dn}}(s) - \gamma_{\mathrm{up},i} \cdot \frac{\mathrm{R_{up}}(s)}{\eta_i}\right)}{s} \tag{11}$$

where η_i is the efficiency of the battery i, and $\gamma_{\mathrm{up},i}$ and $\gamma_{\mathrm{dn},i}$ are battery i's portion of the total up and down regulation capacities. Note that resources providing frequency regulation, including batteries participating in REM, are not required to bid or provide symmetric up and down regulation capacities [8]. Then, the energy level of battery i is

$$E_i(s) = \mathrm{sat_B}(E_{0,i} + E_{\mathrm{NET},i}(s) + E_{\mathrm{REM},i}(s)) \tag{12}$$

where $E_{0,i}$ is the initial energy level of battery i at the start of regulation provision, $E_{\mathrm{REM},i}(s)$ is the energy offset, and

$$\mathrm{sat_B}(x) = \begin{cases} 0, & \text{if } x < 0, \\ x, & \text{if } 0 \le x \le E_{\mathrm{B},i}, \\ E_{\mathrm{B},i}, & \text{if } x > E_{\mathrm{B},i}. \end{cases} \tag{13}$$

where $E_{\mathrm{B},i}$ is the energy capacity of battery i.

The energy offset is delivered at a constant power over each real-time market period of duration 5 min. To calculate the energy offset for each 5-min period t, we first estimate battery i's energy level at the beginning of the period using the estimated energy level 7.5 min prior to the start of the current 5-min period $e_{0,i}(t)$ and the energy offsets scheduled for those 7.5 min, i.e., the offsets in the two periods before the period of interest. Specifically,

$$e_i(t) = e_{0,i}(t) + 0.5 \cdot e_{\mathrm{REM},i}(t-2) + e_{\mathrm{REM},i}(t-1), \tag{14}$$

where we multiply the second term by 0.5 since we only need to consider the energy offset associated with the second 2.5 min of that period. Then, the energy offset is computed as the difference between this estimate and the preferred energy level $e_{\mathrm{pref},i}$, i.e.,

$$e_{\mathrm{REM},i}(t) = e_{\mathrm{pref},i} - e_i(t). \tag{15}$$

3. Simulation Approach and Metrics

We next describe the simulation approach we developed to compute the metrics used to compare the PJM and CAISO strategies. The overall approach is to determine the battery and generator actions at every frequency regulation time step over 24 hours. With this, we can compute the regulation-signal following performance and the additional system control effort.

The first step to determine the battery and generator actions is to compute the system dispatch by solving the AC optimal power flow (OPF) problem co-optimizing

energy and frequency regulation capacity every 5 min. We do not model the day-ahead market or other reserve markets. We assume that the battery under the CAISO strategy only provides frequency regulation, as resources participating in REM are not eligible to participate in the energy market. In PJM, RegD-providing resources are not barred from also participating in the energy market. PJM's controller integrates the RegD signal to calculate the accumulated neutrality bias, but the impacts of battery round-trip efficiency are not captured and so the battery loses charge over time. We assume that the battery under the PJM strategy can participate in the real-time energy market, but for simplicity, we assume that it only does so to manage its SoC. This is a reasonable assumption, as frequency regulation is the primary use for most large-scale batteries [13]. We model the battery under the PJM strategy as a "fixed gen" resource, meaning that it self-schedules in real-time as a price taker [14]. The battery will self-dispatch when the $e_{0,i}(t)$ is below $0.2E_B$ or above $0.8E_B$. The dispatch is calculated according to 14 and 15, but in this case, the energy offset $e_{\mathrm{REM},i}(t)$ is replaced by $e_{\mathrm{PJM},i}(t)$, which represents the energy transacted in the PJM real-time energy market by the battery in time step t.

We also assume the cost of frequency regulation provision by batteries is less than the cost of frequency regulation provision by generators, and so batteries are dispatched at full capacity and do not need to be explicitly included in the OPF formulation. We use the MATPOWER function `runopf_w_res()` [15] which solves

$$\min_{\theta,\mathbf{V},\mathbf{P}_\mathrm{g},\mathbf{Q}_\mathrm{g},\mathbf{R}} \sum_{i\in\mathcal{G}} C_{\mathrm{E},i}(P_{\mathrm{g},i}) + C_{\mathrm{R},i}(R_i) \tag{16}$$

$$\text{s.t. } \mathbf{P}_\mathrm{bus}(\theta,\mathbf{V}) + \mathbf{P}_\mathrm{d} - C_\mathrm{g}\mathbf{P}_\mathrm{g} = 0, \tag{17}$$

$$\mathbf{Q}_\mathrm{bus}(\theta,\mathbf{V}) + \mathbf{Q}_\mathrm{d} - C_\mathrm{g}\mathbf{Q}_\mathrm{g} = 0 \tag{18}$$

$$|S_{\mathrm{f},i}(\theta,\mathbf{V})| \le S_i^{\max}, \quad \forall\, i \in \mathcal{L}. \tag{19}$$

$$|S_{\mathrm{t},i}(\theta,\mathbf{V})| \le S_i^{\max}, \quad \forall\, i \in \mathcal{L} \tag{20}$$

$$V_i^{\min} \le V_i \le V_i^{\max}, \quad \forall\, i \in \mathcal{B}. \tag{21}$$

$$P_{\mathrm{g},i}^{\min} + R_i \le P_{\mathrm{g},i} \le P_{\mathrm{g},i}^{\max} - R_i, \quad \forall\, i \in \mathcal{G}, \tag{22}$$

$$Q_{\mathrm{g},i}^{\min} \le Q_{\mathrm{g},i} \le Q_{\mathrm{g},i}^{\max}, \quad \forall\, i \in \mathcal{G} \tag{23}$$

$$\sum_i R_i \ge R^{\mathrm{req}} \tag{24}$$

where θ is a vector of bus voltage angles, $\mathbf{V}$ is a vector of bus voltage magnitudes, $\mathbf{P}_\mathrm{g}$ and $\mathbf{Q}_\mathrm{g}$ are vectors of generator real and reactive power production, $\mathbf{R}$ is a vector of generator frequency regulation capacities, $\mathcal{G}$ is the set of all generators, $C_{\mathrm{E},i}(P_{\mathrm{g},i})$ is the energy cost function of generator i which depends on generator i's real power output $P_{\mathrm{g},i}$, and $C_{\mathrm{R},i}(R_i)$ is the frequency regulation cost function of generator i which depends on generator i's frequency regulation capacity R_i. Constraints (17) and (18) are nonlinear real and reactive power balance equations, where $\mathbf{P}_\mathrm{bus}(\theta,\mathbf{V})$ and $\mathbf{Q}_\mathrm{bus}(\theta,\mathbf{V})$ are vectors of real and reactive power injections at each bus, $\mathbf{P}_\mathrm{d}$ and $\mathbf{Q}_\mathrm{d}$ are vectors of the real and reactive power demand at each bus, and C_g is a matrix to map generators to their bus location. Constraints (19) and (20) are line flow limits, one for the *from* end and one for the *to* end of each line, where $S_{\mathrm{f},i}(\theta,\mathbf{V})$ and $S_{\mathrm{t},i}(\theta,\mathbf{V})$ represent the apparent power flowing through line i, $S_i^{\max}$ represents the limit in MVA of line i, and $\mathcal{L}$ is the set of all lines. Constraint (21) limits the voltage V_i of bus i, where $V_i^{\min}$ and $V_i^{\max}$ are the voltage limits of bus i and $\mathcal{B}$ is the set of all buses. Constraints (22) and (23) enforce real and reactive power limits of each generator, where $P_{\mathrm{g},i}^{\min}, P_{\mathrm{g},i}^{\max}$ are the real power limits and $Q_{\mathrm{g},i}^{\min}, Q_{\mathrm{g},i}^{\max}$ are the reactive power limits of generator i. Constraint (24) requires the sum of the generators' frequency regulation capacities to meet the generator frequency regulation requirement R^{req}, defined as the system frequency regulation requirement minus the total frequency regulation capacity provided by batteries. Note that frequency regulation capacity is only included in the generator real power limits (22), meaning changes in power flows and voltages caused by actuation of frequency regulation are not constrained by system limits. However, reserve flows usually change voltages and line flows by only small amounts.

The second step to determine the battery and generator actions is to superimpose the frequency regulation actuations onto the dispatch results. For simplicity, we assume that the underlying load is fixed throughout the day, but the system load changes as the battery's load changes according to self-dispatch in PJM and energy offset in CAISO. Specifically, the battery's load is included in the real power demand at the bus where the battery is connected. The battery's load is modeled as a positive demand when the battery is charging and a negative demand when it is discharging. This interaction between the regulation actuation and the real-time energy dispatch requires that the battery's load be updated and the ACOPF problem be re-solved for every 5-min dispatch period. This results in a real-time energy dispatch that changes every 5 min and regulation actuations that change within that 5-min period.

3.1. Regulation signal-following performance

Using the battery actions, we can calculate the regulation signal-following performance by comparing the actions to the frequency regulation signal(s). In practice, PJM and CAISO define their performance scores for frequency regulation differently. CAISO, like many other ISOs, captures a unit's accuracy in signal following by integrating absolute error, as discussed in [16]. PJM incorporates delay, correlation, and accuracy to develop a more complex measure of performance [17]. For simplicity, we use the integration of absolute error between the signal and battery actuation at each time step (i.e., CAISO's approach). We assume that the controls and power electronics of batteries enable them to perfectly follow the signal unless a battery's energy constraints are active.

3.2. Additional system control effort

We use two measures of additional system control effort (ASCE) to quantify how the non-energy constrained resources modify their outputs to manage the energy constraints of the batteries. The first measure of additional system control effort, referred to as ASCE1, is the absolute change in energy produced by the non-energy constrained resources as a result of the energy constraint management strategy.

For the PJM strategy, ASCE1 is the integral of the absolute difference between the RegA signal and what the signal would have been if there were no conditional neutrality feedback

$$\Delta E^{\mathrm{R}}(t) = \int \left| \widetilde{\mathrm{RegA}}(t) - \mathrm{RegA}(t) \right| dt, \qquad (25)$$

added to the difference between the total generator dispatch and what the total generator dispatch would have been without the battery's energy market participation

$$\Delta E^{\mathrm{G}}(t) = \Delta t \sum_{t} \sum_{i} |\widetilde{P_{\mathrm{g},i}}(t) - P_{\mathrm{g},i}(t)|, \qquad (26)$$

where $\widetilde{\cdot}$ denotes a value if there were no conditional neutrality feedback and Δt is the duration of the real-time energy market dispatch interval in seconds.

For the CAISO strategy, ASCE1 is the absolute value of the difference between the total generator dispatch and what the total generator dispatch would have been without REM, i.e., the energy needed for REM plus battery losses. Therefore, it is equal to (26), where $\widetilde{\cdot}$ now denotes the value if there were no REM.

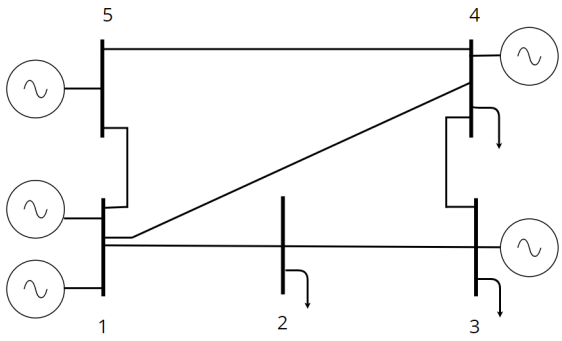

Figure 3. One-line diagram of the PJM 5-bus system without battery.

Table 1. Case Study Parameters

Parameter	Symbol	Value
Proportional Gain	K_{P}	1 (-)
Integral Gain	K_{I}	0.001 (-)
RegA Time Constant	τ_{A}	150 (s)
RegD Time Constant	τ_{D}	10 (s)
CAISO Time Constant	τ	10 (s)
Battery Energy Capacity	E_{B}	1.89 (MWh)
Battery Power Capacity	P_{B}	3 (MW)
Regulation Requirement	R^{req}	5 (MW)
ACE Limit	$\overline{\mathrm{ACE}}$	4 (MW)
Preferred Energy Level	e_{pref}	0.94 (MWh)
Battery Efficiency	η	90 (%)
Time Step	Δt	300 (s)

The second measure of additional system control effort, ASCE2, is the net change in energy produced by the non-energy constrained resources as a result of the energy constraint management strategies. Therefore, to compute ASCE2, we use the same process we used for ASCE1 except we remove the absolute values from (25) and (26).

4. Case Study

We next describe our case study setup and results detailing our comparison on the PJM and CAISO approaches.

4.1. Setup

This section presents a case study in which both strategies are implemented on the PJM 5-bus system (case 5 in MATPOWER [15]) shown in Fig. 3. The case study parameters are given in Table 1. The regulation capacity requirement is typically 0.6-0.9% of the total load [18, 19]. The total load in the MATPOWER case 5 system is 1000 MW. Therefore, the total regulation

capacity (i.e., both RegA and RegD in PJM) was chosen to be 8 MW or 0.8% of the total load. For PJM we assume only batteries provide RegD and only generators provide RegA. As no more than 40% of regulation can be provided by RegD in PJM [20], in both PJM and CAISO we set the amount of regulation provided by the generators in the system to 5 MW and the amount of regulation provided by batteries to 3 MW. A single battery, with specifications representing the average battery serving PJM in 2019 [1] scaled such that the power limit is 3 MW, was included in the system. The battery was placed at Bus 2, though the location was varied to check the sensitivity of the results to the connection point.

The case 5 data was edited to include the 5 MW regulation requirement and enable regulation provision by generators 3 and 5. The other generators were not considered for frequency regulation as they are either dispatched close to their full capacity or not dispatched in the base case. The cost of supplying frequency regulation was set to 1 $/MWh for all participating generators. We assume there is no cost to the battery for providing regulation capacity. We assume that all resources providing regulation offer symmetric capacity.

All modeling and simulation was done in MATLAB and Simulink. The regulation signals for the entire 24 hour period were generated using real ACE data from PJM [21] scaled to fit the 5-bus system. The same ACE data was used for both controllers.

Initial simulations showed windup in the PI controller used by both the PJM and CAISO controllers. We were unable to find information in ISO publications on whether this occurs in real operation and if so, how the ISOs manage it. However, literature suggests that windup is a common issue in the generation of regulation signals [22, 23]. To manage windup in our simulations, we implemented the clamping anti-windup mechanism built into Simulink's PID controller. We tuned the mechanism to find the largest output saturation limit that removed the windup, resulting in limits of [-6,6].

4.2. Results

ACE signal data from [21] corresponding to 14 different 24-hour periods was used to simulate both energy management strategies. The average performance metrics and their standard deviations for each strategy are shown in Table 2. The results suggest that both strategies were able to prevent the battery from reaching its energy constraints. However, the PJM strategy relied on the battery's participation in the real-time energy market in order to be effective over multiple consecutive hours.

Table 2. Average Performance Metrics (and Standard Deviations)

	PJM	CAISO
Performance Score (%)	100.0 (0)	100.0 (0)
ASCE1 (MWh)	5.238 (0.566)	0.941 (0.187)
ASCE2 (MWh)	-3.236 (0.914)	-0.940 (0.189)

In every tested case, the PJM strategy resulted in ASCE metrics with magnitudes significantly larger than those resulting from the CAISO strategy. This indicates that the overall system's energy output deviates further from what it would have been has there been no energy constraints to manage. The net change in energy, corresponding to ASCE2, resulting from both strategies was negative. This means that the non-energy constrained generators decreased their overall energy production in order to manage the energy constraints of the battery. This makes sense, as regulation signals are generally biased in the "lower" direction [20]. Under a "lower" or negative regulation signal, a battery is charging, and so it will subsequently need to be discharged to maintain energy neutrality. Resources that need not operate under energy neutrality, i.e., non-energy constrained resources, must then lower their power output at that later time in order for the net power injection into the system to remain the same.

Under the PJM strategy, the accumulated neutrality bias, $B(s)$ in Fig. 1, is feedback that adjusts the RegA signal at a later time so that the RegD signal can move towards energy neutrality. If the RegD signal has been biased in the negative direction over time, the feedback will lower the RegA signal such that the RegD signal can move in the opposite direction without decreasing the overall effectiveness of the regulation. An example of this is shown in Fig. 4a and Fig. 4b. Under the CAISO strategy, any accumulation or removal of energy in the battery is managed through REM in the energy market. In the case that regulation has been biased in the down direction over time, the battery will have accumulated energy and will need to export it into the energy market. In order for this to happen without changing the net power into the market, the total power output by the other power sources in the system must decrease their output accordingly. Figure 5 shows the power, assumed fixed over each 5-min period, transacted by the battery in the energy market under both the PJM and CAISO strategies. From the figure it can be seen that generally the CAISO battery is injecting power into the energy market to offset energy it has accumulated through regulation provision. It can also be seen that the battery under the PJM strategy purchases power every

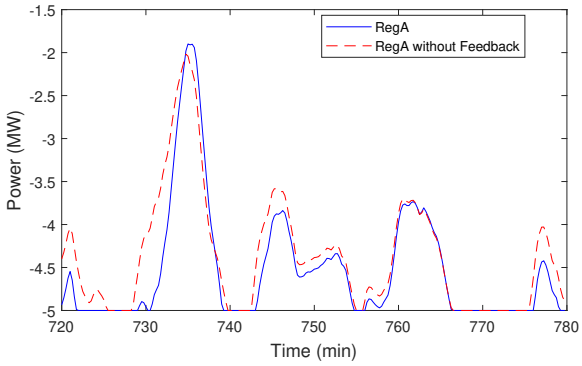

(a)

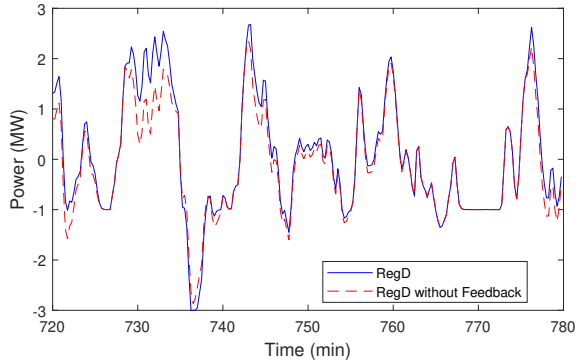

(b)

Figure 4. 4a shows a comparison between the RegA signal generated by the PJM controller and what the RegA signal would have been if there were no feedback. 4b shows the same comparison in terms of RegD. Both figures represents 1 hour of the signal taken from one of the simulated cases.

few hours to recover energy lost due to inefficiency.

It is important to note that while both strategies resulted in a decrease in produced energy, the decrease was significantly larger under the PJM strategy. The experienced decrease in produced power could be a benefit or a detriment, depending on certain factors. For example, if the non-energy constrained generators are polluting fossil fuel generators, then decreasing their power output could decrease pollution. However, the decrease in produced power could also push those generators into less efficient operating ranges, negating the positive environmental impacts of power production reduction and reducing the profitability of providing regulation. More analysis is necessary to establish the effects of the reduction in power production.

To assess whether the battery's location within the system impacts the metrics, the battery was separately modeled at each bus and simulated using the same ACE

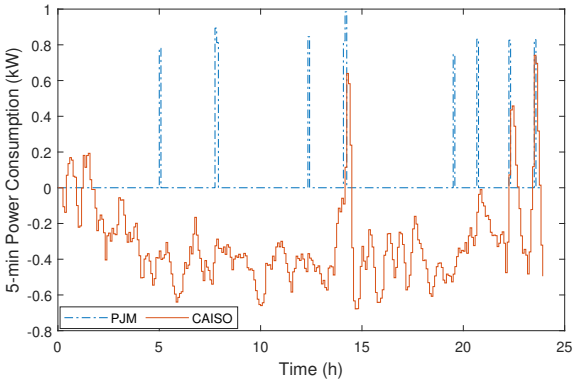

Figure 5. A plot of the fixed power transactions made by the battery in each 5-min real-time market period. A positive value represents power purchased from the market (charging) and a negative value represents power sold to the market (discharging).

data. For both the strategies, the metrics changed only a small amount as we varied battery location, indicating that battery location is insignificant in the comparison of the two strategies.

5. Conclusions

This paper presented a comparison of the strategies used by PJM and CAISO for managing the energy constraints of a battery providing frequency regulation. The case study results suggest that both strategies are sufficient to manage the energy constraints of a battery, but that the PJM strategy requires the battery operator to help manage the battery's SoC by offsetting energy lost due to inefficiency with energy purchased in the real-time energy market. Additionally, the PJM strategy resulted in a larger deviation in total energy production by the non-energy constrained resources when compared to how the system would have operated without any energy constraints to manage. Both strategies resulted in a net power production reduction by non-energy constrained generators, with a larger reduction under the PJM strategy. More analysis is needed to understand whether this reduction is beneficial or detrimental to the system.

A key difference in the structures of the two strategies is the level of responsibility that falls on the ISO. Under the CAISO strategy, the ISO is entirely responsible for managing the SoC of a resource under REM. This requires that CAISO must obtain information regarding SoC, efficiency, and/or other pertinent information on a regular basis for every resource participating in REM. PJM, on the other hand, leaves some of the responsibility up to the

energy constrained resource operator. Under regular operation, PJM's conditional neutrality controller can be run autonomously and only requires information internal to the ISO. Managing energy constraints in PJM relies partially on the battery operator, but the operator is incentivized to manage SoC through performance dependent regulation payment. ISOs should consider the trade-off between the level of effort/communication required on their part when making design decisions regarding market mechanisms for managing energy-constrained resources.

Another consideration to make when evaluating the advantages and disadvantages of these two strategies are their implications for overall system resource mix needs. For example, the PJM strategy requires resources which are capable of following the RegA signal, a signal which is generally not energy neutral. This indicates that in its current implementation, there are limitations on how much of the regulation service can be provided by energy-limited resources. Currently, PJM limits procurement of the RegD service to 40% of its regulation needs [20]. Under the CAISO strategy, all regulation services could potentially be provided by batteries or other energy-limited resources.

There were a number of assumptions made during the controller design and implementation process that may not accurately represent the ISOs' implementations. These assumptions were made to fill in gaps in the documentation of these approaches. For example, little information on how CAISO derives regulation signals from ACE could be found, so it was assumed that the time constant of the low-pass filter was the same as the time constant in the low-pass filter for the RegD signal. In the PJM controller, it was assumed that the ACE magnitude at which conditional neutrality would be suspended was 4 MW, which is approximately the 90-percentile of the scaled ACE data used. Without adequate knowledge of the true implementations, sensitivity analysis should be done to assess the importance of these design parameters.

Another limitation of this work is that only a small test system was used. Implementation on the MATPOWER case 9 system, a 9-bus system, gave similar results. In future work, more realistic system sizes and topologies should be tested to assess their effects on the results.

Additional future work on this topic will be to investigate the merits and drawbacks of the two outlined strategies for managing battery energy constraints from the perspective of the battery owner. The owner of a battery providing frequency regulation would want to know which strategy would result in the greatest profit and/or the smallest level of degradation.

References

[1] U.S. Energy Information Administration, "Battery storage in the United States: An update on market trends." https://www.eia.gov/analysis/studies/electricity/batterystorage/pdf/battery_storage_2021.pdf, 2021.

[2] T. Bowen, I. Chernyakhovskiy, and P. Denholm, "Grid-scale battery storage: Frequently asked questions." https://www.nrel.gov/docs/fy19osti/74426.pdf, 2019.

[3] A. Ingalalli, A. Luna, V. Durvasulu, T. M. Hansen, R. Tonkoski, D. A. Copp, and T. A. Nguyen, "Energy storage systems in emerging electricity markets: Frequency regulation and resiliency," in *IEEE Power Energy Society General Meeting (PESGM)*, 2019.

[4] R. Sioshansi, P. Denholm, and T. Jenkin, "Market and policy barriers to deployment of energy storage," *Economics of Energy & Environmental Policy*, vol. 1, no. 2, pp. 47–64, 2012.

[5] O. Leitermann, *Energy storage for frequency regulation on the electric grid*. PhD thesis, Massachusetts Institute of Technology, 2012.

[6] PJM, "Implementation and rationale for PJM's conditional neutrality regulation signals." https://www.pjm.com/~/media/committees-groups/task-forces/rmistf/postings/regulation-market-whitepaper.ashx#:~:text=The%20conditional%20neutrality%20controller%20is,charge%20of%20Regulation%20D%20resources, 2017.

[7] CAISO, "Non-generator resource (NGR) and regulation energy management (REM) overview – phase 1." http://www.caiso.com/Documents/NGR-REMOverview.pdf, 2014.

[8] CAISO, "Regulation energy management draft final proposal." https://www.caiso.com/Documents/RevisedDraftFinalProposal-RegulationEnergyManagement-Jan13_2011.pdf, 2011.

[9] M. Kintner-Meyer, "Regulatory policy and markets for energy storage in North America," *Proceedings of the IEEE*, vol. 102, no. 7, pp. 1065–1072, 2014.

[10] C. A. Agostini, F. A. Armijo, C. Silva, and S. Nasirov, "The role of frequency regulation remuneration schemes in an energy matrix with high penetration of renewable energy," *Renewable Energy*, vol. 171, pp. 1097–1114, 2021.

[11] L. Meng, J. Zafar, S. K. Khadem, A. Collinson, K. C. Murchie, F. Coffele, and G. M. Burt, "Fast frequency response from energy storage systems—a review of grid standards, projects and technical issues," *IEEE Transactions on Smart Grid*, vol. 11, no. 2, pp. 1566–1581, 2020.

[12] C. Loutan, V. Gevorgian, S. Chowdhury, M. Bosanac, and E. Kester, "Avangrid Renewables Tule Wind Farm: Demonstration of capability to provide essential grid services." http://www.caiso.com/documents/windpowerplanttestresults.pdf, 2020.

[13] International Renewable Energy Agency, "Electricity storage and renewables: Costs and markets to 2030." https://www.climateaction.org/images/uploads/documents/IRENA_Electricity_Storage_Costs_2017.pdf, 2017.

[14] L. Walter, "PJM energy storage participation model: Energy market." https://www.pjm.com/-/media/committees-groups/committees/mic/20190315-special-esrco/20190315-item-03a-electric-storage-resource-model.ashx, 2019.

[15] R. D. Zimmerman, C. E. Murillo-Sánchez, and R. J. Thomas, "MATPOWER: Steady-state operations, planning, and analysis tools for power systems research and education," *IEEE Transactions on Power Systems*, vol. 26, no. 1, pp. 12–19, 2011.

[16] B. Xu, Y. Dvorkin, D. S. Kirschen, C. A. Silva-Monroy, and J.-P. Watson, "A comparison of policies on the participation of storage in U.S. frequency regulation markets," in *IEEE Power and Energy Society General Meeting (PESGM)*, 2016.

[17] PJM, "PJM manual 12: Balancing operations." https://www.pjm.com/~/media/documents/manuals/m12.ashx, 2020.

[18] PJM, "Regulation market data." https://dataminer2.pjm.com/feed/reg_market_results, 2022. Last accessed 1 April 2022.

[19] PJM, "Hourly load: Metered." https://dataminer2.pjm.com/feed/hrl_load_metered, 2022. Last accessed 1 April 2022.

[20] T. Lee, "Energy storage in PJM: Exploring frequency regulation market transformation." https://kleinmanenergy.upenn.edu/wp-content/uploads/2020/08/Energy-Storage-in-PJM_0-1.pdf, 2017.

[21] PJM, "Area control error." https://dataminer2.pjm.com/feed/area_control_error, 2022. Last accessed 1 April 2022.

[22] W. Ma and B. Xu, "A data-driven nonlinear recharge controller for energy storage in frequency regulation," in *IEEE Power & Energy Society General Meeting*, pp. 1–5, 2021.

[23] E. N. Sofia Guzman, M. Arriaga, C. A. Cañizares, J. W. Simpson-Porco, D. Sohm, and K. Bhattacharya, "Regulation signal design and fast frequency control with energy storage systems," *IEEE Transactions on Power Systems*, vol. 37, no. 1, pp. 224–236, 2022.